COMPACT CIRCULARLY POLARIZED SLOT-RING ANTENNA AND

MICROSTRIP BANDPASS FILTER USING TRIANGULAR OPEN-

LOOP RESONATORS

A Thesis

by

MUHAMMAD FAHAD FAROOQUI

Submitted to the Office of Graduate Studies of
Texas A&M University
in partial fulfillment of the requirements for the degree of

MASTER OF SCIENCE

December 2006

Major Subject: Electrical Engineering

COMPACT CIRCULARLY POLARIZED SLOT-RING ANTENNA AND

MICROSTRIP BANDPASS FILTER USING TRIANGULAR OPEN-

LOOP RESONATORS

A Thesis

by

MUHAMMAD FAHAD FAROOQUI

Submitted to the Office of Graduate Studies of
Texas A&M University
in partial fulfillment of the requirements for the degree of

MASTER OF SCIENCE

Approved by:

Chair of Committee,   Kai Chang
Committee Members, Gregory Huff
                             Edgar Sanchez-Sinencio
                             Kenith Meissner
Head of Department, Costas Georghiades

December 2006

Major Subject: Electrical Engineering

ABSTRACT

Compact Circularly Polarized Slot-Ring Antenna and Microstrip Bandpass Filter Using

Triangular Open-Loop Resonators. (December 2006)

Muhammad Fahad Farooqui, B.E., NED University

Chair of Advisory Committee: Dr. Kai Chang

In this thesis two different research topics are undertaken, both in the area of compact RF/microwave circuits design. The first topic involves the design of a compact circularly polarized (CP) slot-ring antenna. A study of several compact CP microstrip and slotline antennas reported in the past has been carried out. In this research, a method of reducing the size of a printed slot-ring antenna is proposed. The reduction in size is achieved by introducing meandered-slot sections in the ring. Circular polarization is achieved by introducing an asymmetry, also a meandered-slot section, and feeding the antenna at an angle of 45° from the asymmetry using a microstrip feed line. The minimum axial ratio of 0.4 dB is obtained at 2.46 GHz, which is the operating frequency of the antenna. The size of the proposed antenna is reduced by about 50% compared to a conventional CP slot-ring antenna and it displays a CP bandwidth of about 2.5%. The simulated and measured results are presented, and they are in good agreement. The small size of the antenna makes it very suitable for use in modern RF/microwave wireless systems which require compact, low cost, and high performance circuits. Moreover, its CP behavior makes it more attractive for applications such as satellite communications.

The second topic in the thesis involves the design of a compact microstrip bandpass filter using triangular open-loop resonators. A new compact three-pole microstrip bandpass filter using four triangular open-loop resonators is presented. A fourth resonator is placed to provide cross-coupling in the structure which gives a better skirt rejection. The measured pass-band center frequency is 2.85 GHz. The filter demonstrates about 7% bandwidth with insertion loss of less than 1 dB in the passband, a return loss of greater than 15 dB and out-of-band rejection of greater than 30 dB. The simulated and measured results are in good agreement. The proposed filter is very attractive for use in modern wireless systems which require bandpass filters having compact size, low insertion loss, high selectivity, and good out-of-band rejection.

ACKNOWLEDGMENTS

TABLE OF CONTENTS

TABLE OF CONTENTS

Page

LIST OF FIGURES

LIST OF FIGURES

LIST OF TABLES

CHAPTER I

INTRODUCTION

Recent growth in mobile communications has created a need for miniaturized circuits compatible with microwave and millimeter wave integrated circuits (MICs) and monolithic microwave integrated circuits (MMICs). This thesis comprises two different research topics, both in the area of compact RF/microwave circuit design. The first topic involves the design of a compact circularly polarized (CP) meandered slot-ring antenna. The second topic in the thesis involves the design of a compact microstrip bandpass filter using triangular open-loop resonators.

Chapter II describes the research on the design of a compact CP slot-ring antenna. Advantages of slot-ring antenna over conventional microstrip ring antenna are discussed. A brief analysis of slot-ring resonator is presented including the various methods to feed the slot-ring structure. The analysis is followed by a review of several compact CP microstrip and slotline antennas that have been reported in the past. The proposed geometry of the antenna is presented. Finally the measured and simulated results of the proposed antenna are presented and discussed.

_____

This thesis follows the style of *IEEE Transactions on Microwave Theory and Techniques*.

Chapter III covers the design of a compact microstrip bandpass filter using triangular open-loop resonators. The chapter starts with a brief discussion on the applications of compact microstrip bandpass filters. A review of microstrip bandpass filters using triangular resonators reported in the past is carried out followed by the design method of the proposed bandpass filter. The chapter ends with a discussion on the simulated and measured results of the proposed filter.

Chapter IV summarizes the research done in this thesis. Some improvements that can be done in the designs are suggested along with some recommendations about future work that can done in the area.

CHAPTER II

COMPACT CIRCULARLY POLARIZED SLOT-RING ANTENNA

2.1 Introduction

The recent growth in mobile communication has created a need for miniaturized antennas for practical use. Microstrip antennas have the advantages of small size, low cost, and planar structure, which is compatible with microwave integrated circuits (MICs) and monolithic microwave integrated circuits (MMICs). However when used in mobile communication products, the problem encountered is their limited bandwidth. This problem can be solved to some extent by using printed slot antennas which usually have a wider impedance bandwidth than microstrip antennas [1-3]. By introducing asymmetry in the slot structure, circular polarization can be obtained which is beneficial for many applications (e.g., satellite, terrestrial communications) as it eliminates the requirement of aligning the electrical field vector at receiver and transmitter.

In this research, a new miniaturized circularly polarized (CP) slot-ring antenna is presented. The reduction in size is achieved by utilizing the inner area of the ring to form meandered-slot sections. With the introduction of some asymmetry or perturbation in the structure of a single feed microstrip ring antenna, it is possible to excite two orthogonal modes for CP operation [4]. Since printed slot-ring antenna is the dual of a ring microstrip antenna, the same principle can be applied to make it CP [1-3]. The asymmetry used here is also a meandered-slot section with smaller slot width compared

to that of the ring [1]. The antenna is fed by microstrip line at an angle of 45° from the asymmetry. A prototype of the design is simulated and implemented. The simulation of the proposed antenna is carried out using IE3D software. The measured and simulated results are in good agreement.

2.2 Slotline ring analysis

The slotline ring resonator was first proposed by Kawano and Tomimuro [5] for measuring the dispersion characteristics of slotline. The slot-ring structure is the mechanical dual of the more familiar microstrip ring resonator. The comparison is given in Fig. 1 [6]. The microstrip ring is a segment of microstrip bent into a loop; slot ring is a segment of slotline bent into a loop. Analysis of slot ring antenna can be found in [6]. To use the structure as an antenna, the first order mode is excited as shown in Fig. 2 (a), and the impedance seen by the voltage source will be real at resonance. All the power delivered to the ring will be radiated [6]. Following the analysis by Stephan et al. [6], the resonant frequency, the far field radiation patterns, and the input impedance at the feed point can be calculated.

A first order estimate of the resonant frequency can be derived from the transmission line equivalent circuit of the slot-ring. Since the structure is symmetrical, a magnetic wall can be placed across the ring as shown in Fig. 3(a) [6]. This operation yields the
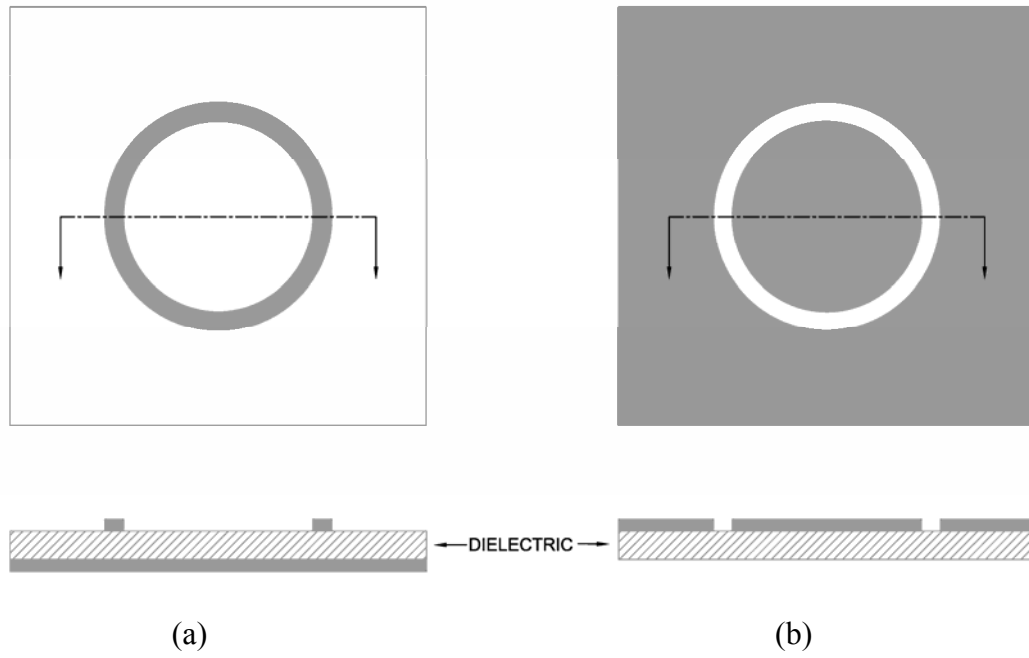
Fig. 1. Comparison of (a) microstrip ring and (b) slot-ring structures.
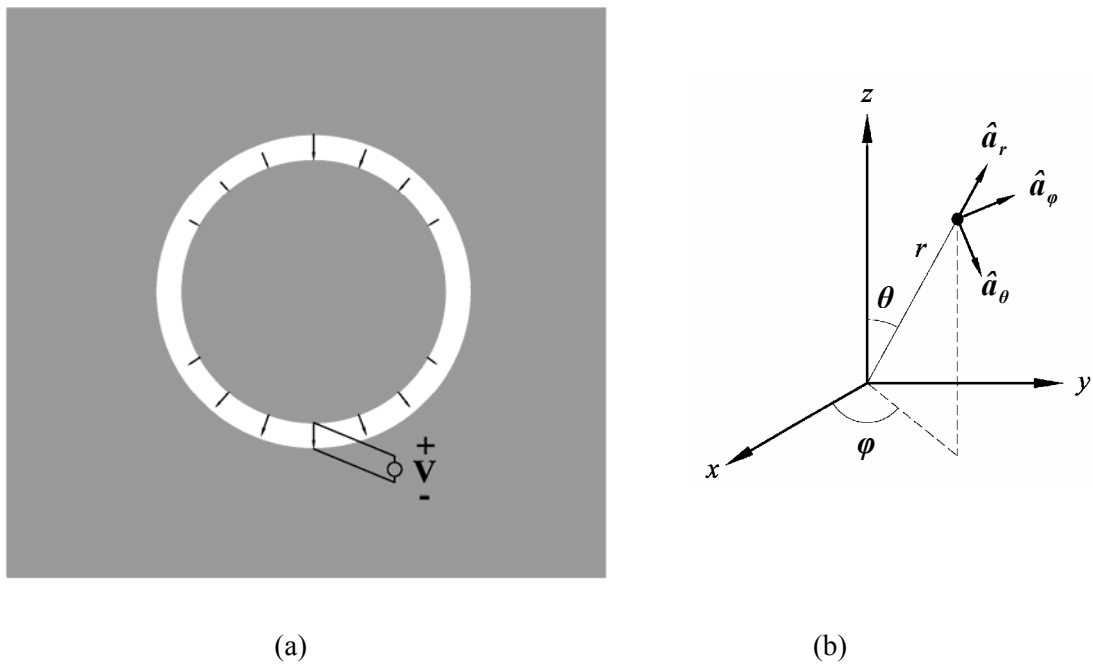
Fig. 2. (a) Slot-ring feed method showing electric field. (b) Standard spherical coordinates.
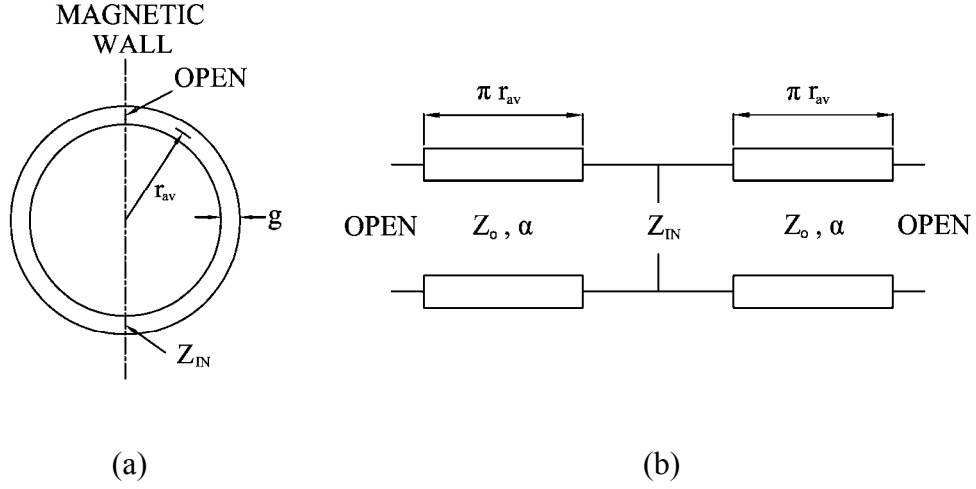
Fig. 3. Transmission-line equivalent circuit of slot-ring antenna. (a) With magnetic wall across slot-ring. (b) Resulting transmission-line equivalent circuit.

equivalent transmission-line equivalent circuit as shown in Fig. 3(b). At the resonant frequency of the first-order mode, the two lines are each half wavelength long electrically. Knowledge of the mechanical length and the velocity factor allows the calculation of resonance to within 10 to 15 percent of the true frequency [6]. The smaller the relative gap g / r_{av}, the better the estimate will be. Using the standard spherical coordinates r, θ and φ, shown in Fig. 2(b), to refer to the point at which the fields are measured, the far-field equations are [6]

$$E_\theta(r,\theta,\phi) = -k_o \frac{e^{jk_o r}}{r} \frac{j^n e^{jn\phi}}{2}[\widetilde{E}_o(k_o \sin\theta)] \tag{1}$$

$$E_\theta(r,\theta,\phi) = +k_o \frac{e^{-jk_o r}}{r} \frac{j^{n+1} e^{jn\phi}}{2} \cos\theta[\widetilde{E}_e(k_o \sin\theta)] \tag{2}$$

Where $k_o = \omega\sqrt{\mu_o \varepsilon_o}$ and the linear combination of Hankel-transformed estimates are used

$$E_o(k_o \sin\theta) = \widetilde{E}_{(+)}(k_o \sin\theta) - \widetilde{E}_{(-)}(k_o \sin\theta) \tag{3}$$

$$E_e(k_o \sin\theta) = \widetilde{E}_{(+)}(k_o \sin\theta) + \widetilde{E}_{(-)}(k_o \sin\theta) \tag{4}$$

Where the (n±1)th-order Hankel transforms are defined by

$$\widetilde{E}_{(\pm)}(\alpha) = \int_{r_i}^{r_a} J_{n\pm1}(\alpha r)dr \tag{5}$$

Where $J_n(\alpha r)$ is the nth-order Bessel function of the first kind, α is the Hankel-transform variable, and r_i and r_a are the inner and outer ring radii, respectively. These integrals can be evaluated analytically using tables. At the center of the ring, r=0, n is the order of resonance being analyzed. In the case of interest, n=1 and $\omega=\omega_o$=the resonant frequency. For the finite thickness of the dielectric substrate, the preceding equations need to be modified for better accuracy [6]. The input impedance at the feed point can be calculated by [6]:

$$Z_{in} = \frac{[\ln(\frac{r_a}{r_i})^2]}{P} \tag{6}$$

Where P is the power given by

$$P = \iint_{sphere} \frac{\frac{1}{2}\sqrt{|E_\theta|^2 + |E_\phi|^2}}{Z_{fs}} ds \tag{7}$$

Where Z_{fs} is the intrinsic impedance of free space. The slotline resonator has also been analyzed using distributed transmission line model [7], spectral domain analysis [8], and Babinet's equivalent circular loop [9]. The distributed transmission line method provides a simple and straight-forward solution.

Coupling between the external feed lines and slotline ring can be classified into the following three types:

(1) Microstrip coupling

(2) CPW coupling

(3) Slotline coupling

Fig. 4 shows these three possible coupling schemes. Microstrip coupling that utilizes the microstrip-slotline transition is a capacitive coupling. The lengths of input and output microstrip coupling stubs can be adjusted to optimize the loaded-Q values. However, less coupling may affect the coupling efficiency and cause higher insertion loss. The trade-off between the loaded-Q and coupling loss depends on the applications.

The CPW-coupled slotline ring resonator using CPW-slotline transition is also a capacitively coupled ring resonator. The CPW coupling is formed by a small coupling gap between the external CPW feed lines and the slotline ring. The loaded-Q value and insertion loss are dependent on the gap size. This type of slotline ring resonator is truly planar and also allows easy series and shunt device mounting.

The slotline ring coupled to a slotline feed is an inductively coupled ring resonator. The metal gaps between the slotline ring and the external slotline feeds are for the coupling of magnetic field energy. Therefore, the maximum electric field points of this resonator are opposite to those of the capacitively coupled slotline ring resonator. Hence slotline fed slot-ring is the dual of the microstrip fed slot-ring.

MICROSTRIP

CPW
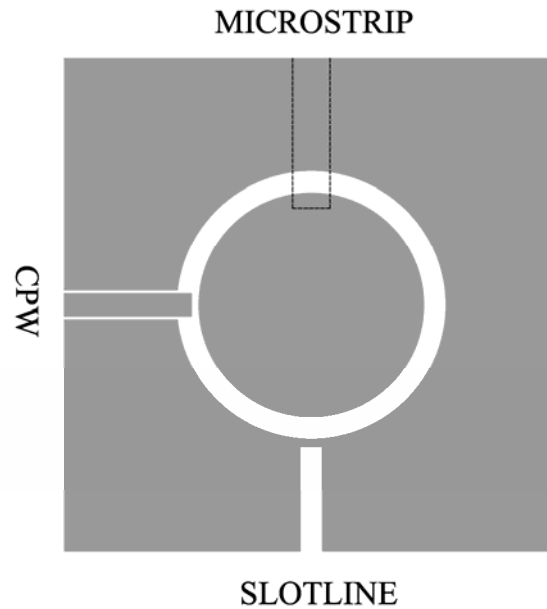
SLOTLINE

Fig. 4. Three possible feed configurations for the slotline ring resonator.

2.3 Review of various microstrip and slotline CP antennas

In order to obtain CP radiation pattern from the slotline ring antenna, two orthogonal degenerate modes need to be excited in the structure. Wolff [10] first reported the degenerate modes in a microstrip ring resonator by using asymmetric feed lines or notch perturbation. Since the slot-ring structure is the dual of the microstrip ring, it is also possible to excite degenerate modes in the slot-ring by introduction of some asymmetry or perturbation in order to obtain circularly polarized radiation pattern.

Fig. 5 shows various CP microstrip and slotline antenna configurations. A CP printed antenna is categorized into two types based upon the number of feeding points required

for CP excitation: one is dual feed CP antenna with an external polarizer such as 3 dB hybrid or offset-feeding line, and the other is a singly fed one without a polarizer. The dual-feed configuration require an external power divider, as shown in Fig. 5(a), or offset-feeding lines, as shown in Fig. 5(b), with one quarter wavelength long than the other. The use of offset feeding lines has a major disadvantage of narrow bandwidth, since the frequency dependency of an offset-feeding line is greater than that of the usual hybrid. Several power dividers that have been successfully employed for CP generation include quadrature hybrid, the ring hybrid, Wilkinson power divider and the T-junction power splitter.

CP radiation can also be obtained by using only a single feed thereby eliminating the need for a power divider network. Such configuration involves slightly perturbing the antenna structure at appropriate locations with respect to the feed to excite orthogonal modes. Several types of perturbations have been reported to obtain CP antenna. Fig. 5(c) shows a circular microstrip antenna having two notches at -45° and 135° from the feed point [11]. Fig. 5(d) shows a microstrip CP ring antenna in which an ear is used as a perturbation at the outer periphery [12]. A microstrip-feed proximity-coupled ring antenna is presented in [13]. The perturbations for CP operation are produced by adding two inner stubs as shown in Fig 5(e). Feeding by proximity coupling from microstrip line has the advantages of increasing the impedance bandwidth and reducing radiation from the feeding network. A square patch antenna can be made CP by truncating its corners as shown in Fig. 5(f), or by loading it by a diagonal slot at the center as shown in

HYBRID

RHCP   LHCP

RHCP   LHCP

(a)
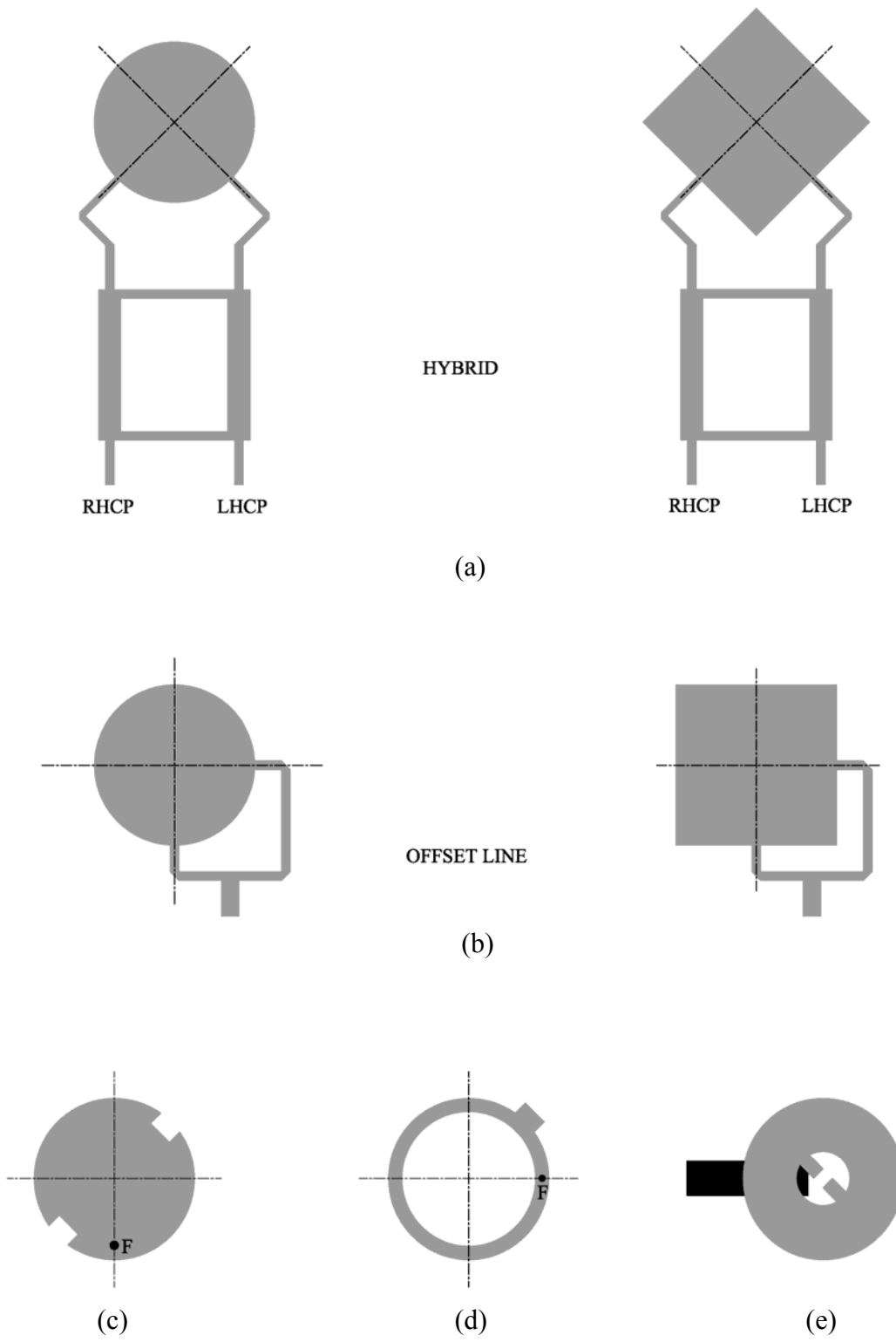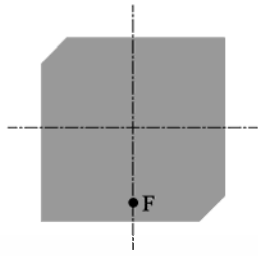
OFFSET LINE

(b)

F

F

(c)   (d)   (e)
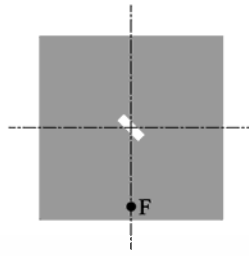
Fig. 5. Various microstrip and slotline CP antenna configurations.

(f)

(g)
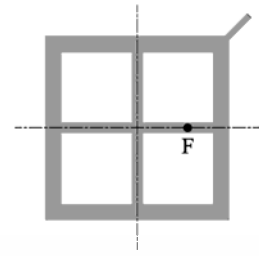
(h)
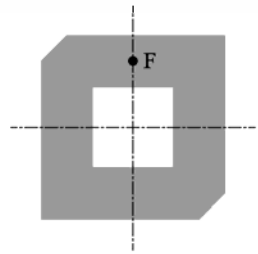
(i)
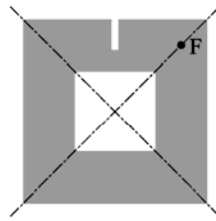
(j)
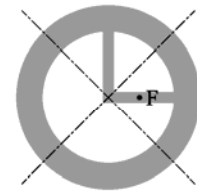
(k)
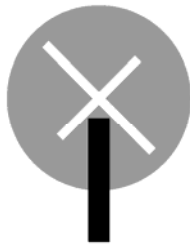
(l)

(m)

(n)

Fig. 5(continued).

(o)

(p)

(q)

(r)

(s)

(t)

(u)

Fig. 5(continued).

(v)
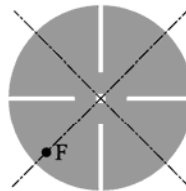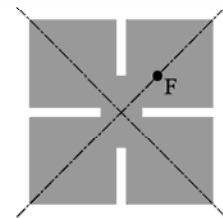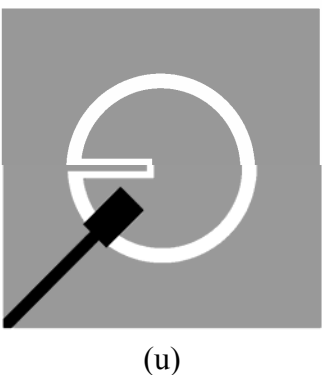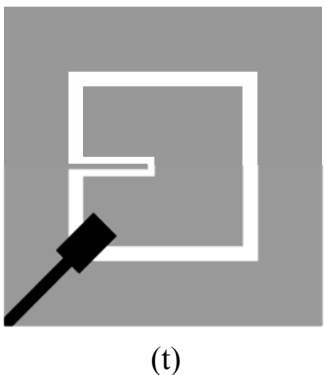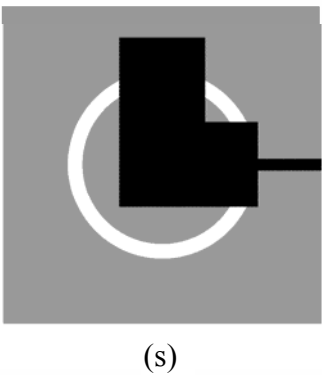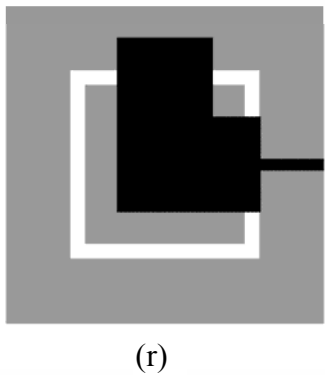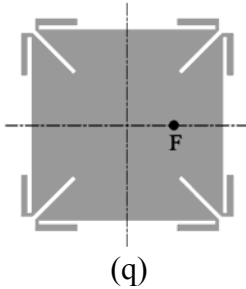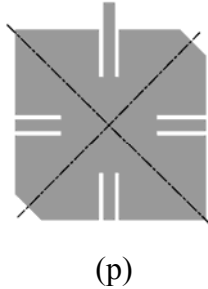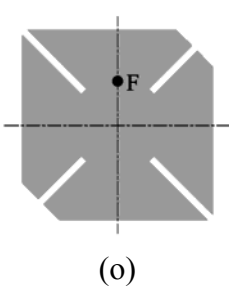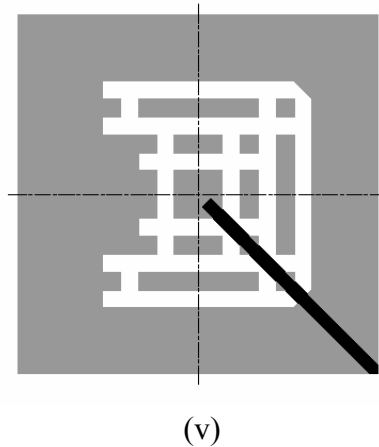
Fig. 5(continued).

Fig. 5(g) [14]. A new design of a square-ring microstrip antenna with a cross strip and small tuning stub for achieving compact CP operation is proposed in [15]. The cross strip can be placed on the center lines as shown in Fig. 5(h), or diagonals of the square ring patch. Similar to square patch of Fig. 5(f), a square ring can also be made compact CP antenna by truncating its corners as shown in Fig. 5(i) [16]. By introducing a narrow slit on the outer periphery of a square-ring structure [17], shown in Fig. 5(j), CP pattern can also be obtained. Fig. 5(k) shows an annular-ring antenna with an L-shaped strip placed inside the ring to make it CP [18]. A circular disc loaded with a cross slot has been reported by Iwasaki [19]. In this configuration, shown in Fig. 5(l), two slots of unequal length cross orthogonally at the center of each other which is also the center of the disc. The antenna is fed by a proximity-coupled microstrip feed line. A circular disc loaded with four slots has also been developed by Bokhari et al. [20] for circular polarization as shown in Fig. 5(m). A slit loaded square patch antenna is shown in Fig

5(n), in which the square patch is loaded with two pair of slits to reduce the antenna size and make it CP [21], similar to the slit loaded disc of Fig. 5(m). Fig. 5(o) shows a compact CP square microstrip antenna with four slits and a pair of truncated corners [22]. CP design of inset microstripline-fed microstrip antenna with three pairs of slits is proposed in [23] and shown in Fig. 5(p). Cutting slots and adding tails, make the square patch antenna small as well as CP [24]. By changing the lengths of the tails along one diagonal axis, the antenna can be excited effectively for circular polarization. The antenna structure is shown in Fig. 5(q).

Recently, various CP designs of slotline antenna have been proposed. Fig 5(r) and 5(s) show square and circular slot-ring antennas fed by a series microstrip line. The series microstrip line couples the two orthogonal sides of the ring to obtain CP pattern [2,3]. Utilizing the duality between microstrip ring and slotline ring structures, a CP design of slot-ring antenna has also been proposed in [1] by introducing asymmetry in the slot structure and feeding the antenna at an angle of 45° from the asymmetry using a microstrip feed line. The proposed asymmetry is in the form of a meandered slot section as shown in Fig. 5(t) and Fig. 5(u). A new type of CP slot antenna is proposed by Ghali et al. [25]. The design utilizes "island-like" space filling curves and proper asymmetry to achieve broad-band CP operation. The antenna structure is shown in Fig. 5(v).

The performance of the various antenna configurations discussed above is summarized in Table 1.

Table 1. Performance of various microstrip and slotline CP antennas.

[Reference] Fig.	Transmission Line	Resonant Frequency	CP Bandwidth	Peak Gain	Size Reduction	Substrate (H) thickness (ε_r) Dielectric constant
[11] Fig. 5(c)	Microstrip	1.53 GHz	0.7 %	6.7 dBi	-	H=5 mm, ε_r=1
[12] Fig. 5(d)	Microstrip	4.85 GHz	3 - 4 % *	-	-	H=1.59 mm, ε_r=2.52
[13] Fig. 5(e)	Microstrip	6.3 GHz	1 %	-	-	H=0.8 mm, ε_r=2.33
[14] Fig. 5(f)	Microstrip	3.175 GHz	0.925 % *	-	-	H=125 mils, ε_r=2.52
[14] Fig. 5(g)	Microstrip	3.13 GHz	1.214 % *	-	-	H=125 mils, ε_r=2.52
[15] Fig. 5(h)	Microstrip	1.695 GHz	0.89 %	-	33 %	H=1.6 mm, ε_r=4.4
[16] Fig. 5(i)	Microstrip	2.33 GHz	1.37 %	-	19 %	H=1.6 mm, ε_r=4.4
[17] Fig. 5(j)	Microstrip	2.18 GHz	1.1 %	-	19 %	H=1.6 mm, ε_r=4.4
[18] Fig. 5(k)	Microstrip	2.51 GHz	2 %	8 dBi	-	H=0.8 mm, ε_r=4.4
[19] Fig. 5(l)	Microstrip	1.55 GHz	0.65 %	6 dBi	36 % in radius.	H=2.6 mm, ε_r=4.4
[20] Fig. 5(m)	Microstrip	-	-	-	-	H=1.52 mm, ε_r=2.5
[21] Fig. 5(n)	Microstrip	1.849 GHz	1.3 %	-	36 %	H=1.6 mm, ε_r=4.4

Table 1 (continued).

[Reference] Fig.	Transmission Line	Resonant Frequency	CP Bandwidth	Peak Gain	Size Reduction	Substrate (H) thickness (ε_r) Dielectric constant
[22] Fig. 5(o)	Microstrip	2.262 GHz	0.84 %	2.8 dBi	36 %	H=1.6 mm, ε_r=4.4
[23] Fig. 5(p)	Microstrip	1.653 GHz	0.7 %	-	55%	H=1.6 mm, ε_r=4.4
[24] Fig. 5(q)	Microstrip	2.492 GHz	0.382 %	4.6 dBi	50%	H=1.524 mm, ε_r=3.367
[2] Fig. 5(r)	Slotline	2.695 GHz	6.1 %	3.3 dBi	-	H=1.6 mm, ε_r=4.4
[3] Fig. 5(s)	Slotline	2.41 GHz	3.4 %	3.9 dBi	-	H=1.6 mm, ε_r=4.4
[1] Fig. 5(t)	Slotline	1.56 GHz	4.3 %	4.3 dBi	-	H=1.6 mm, ε_r=4.4
[1] Fig. 5(u)	Slotline	1.72 GHz	3.5 %	3.8 dBi	-	H=1.6 mm, ε_r=4.4
[25] Fig. 5(v)	Slotline	2.8 GHz	22 %	-	-	H=1.52 mm, ε_r=3.5

---

* Indicates CP bandwidth for axial ratio < 6 dB. The remaining CP bandwidths are for axial ratio < 3 dB.

2.4 Antenna design

The review of microstrip and slotline CP antennas in the preceding section shows that not much work has been reported on the design of compact slotline CP antennas as compared to microstrip CP antennas despite of the fact that slotline antennas provide much greater impedance and CP bandwidth than microstrip antennas . This research provides the design of a compact CP slotline ring antenna. Fig. 6 shows the geometry of the proposed antenna along with the actual dimensions. The antenna is fabricated on Rogers RT/Duroid 5880 substrate with thickness (H) of 31 mils and relative dielectric constant (ε_r) of 2.2. The slot width W_1 is fixed to be 1 mm. The meandered-slot sections have length L_1 and width D_1. The asymmetry in the ring, also a meandered-slot section similar to the one in Fig. 5(u) [1], has length L_2, width D_2 and slot width W_2. The operating frequency of the slot-ring antenna is the frequency whose guided-wavelength is approximately equal to the mean circumference of the ring [1,2,26]. Slot guided-wavelength can be found by [4]

$$\lambda_{gs} = \lambda_o \left[1.045 - 0.36 \ln\varepsilon_r + \frac{6.3 W_1 \varepsilon_r^{0.945}}{H(238.64 + 100 W_1/H)} - \left\{ 0.148 - \frac{8.81(\varepsilon_r + 0.95)}{100\varepsilon_r} \right\} \ln\left(\frac{H}{\lambda_o} \right) \right]$$

(8)

Where λ_o is the free space wavelength and W_1 is the slotline width. Hence the resonant frequency f of the antenna is given by

$$f = \frac{c}{\lambda_{gs}}$$

(9)
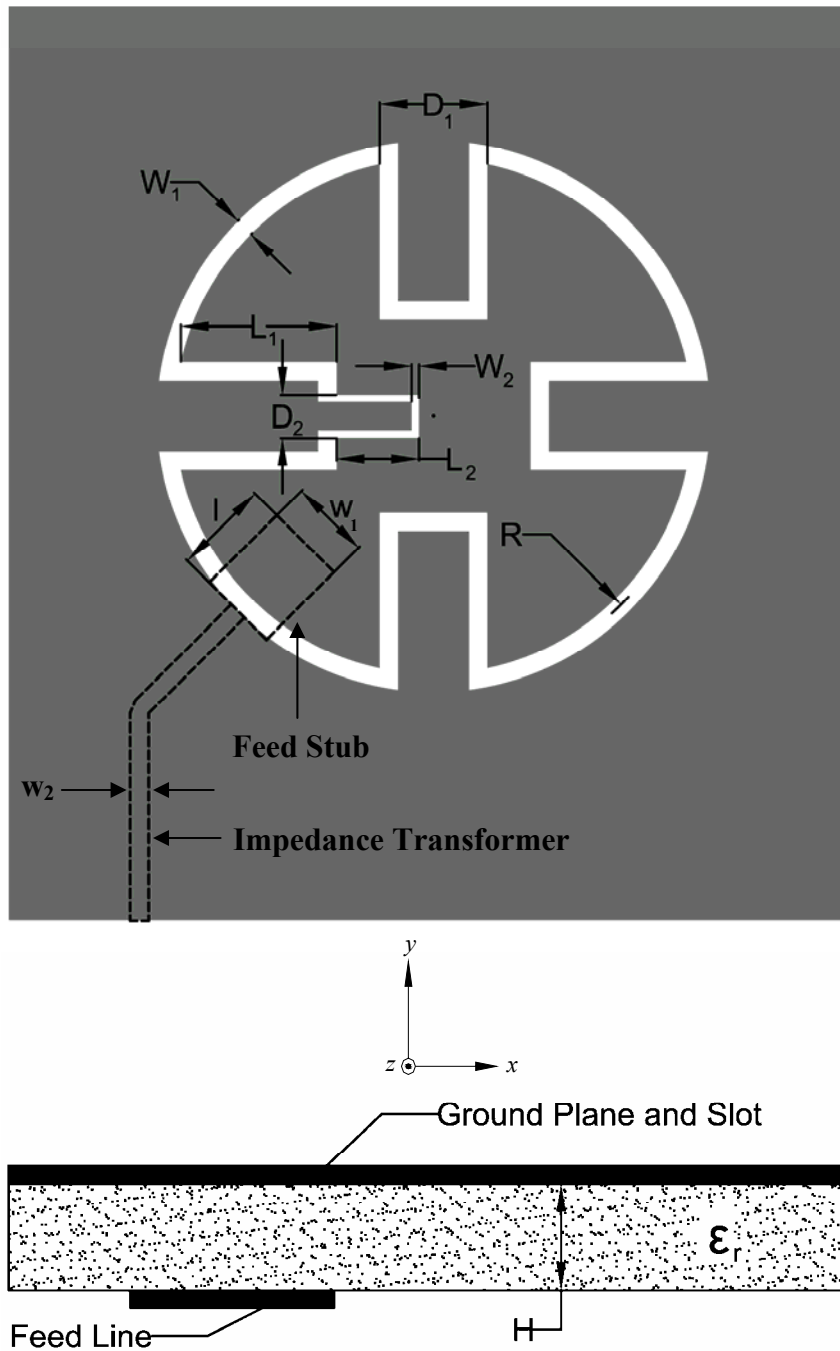
Fig. 6. Geometry of the proposed meandered slot-ring antenna: W_1=1 mm, W_2= 0.2 mm, L_1=7.3 mm, L_2=3.3 mm, D_1= 4mm, D_2=1.2 mm, R=11.5 mm, w_1=4.5 mm, l=1.8 mm and w_2=0.5 mm.

Where c is the speed of light in free space. In [1], however, the resonant frequency was obtained by taking the circumference of the slot-ring equal to the free space wavelength of the resonant frequency and using a correction factor to account for different dielectric media on the two sides of the slot antenna. This approach does not provide good approximation in finding the resonant frequency of the proposed antenna. For the proposed antenna, the total length of the slot-ring along with the meandered sections is approximately $2\pi R + 8L_1$.

The antenna is fed by a microstrip line at an angle of 45° from the asymmetry to obtain circular polarization. The microstrip feed line is composed of a feed stub of length l and width w_1 and a quarter-wavelength transformer of width w_2. The dimensions of the feed stub are fine adjusted to obtain the optimal impedance bandwidth looking at the edge of the ring as oppose to [1] where the feed stub is connected to 50 Ω line and simply has twice its width to improve coupling. The length L_2 of the asymmetry is also fine adjusted to obtain minimum axial ratio and optimal CP bandwidth. To achieve impedance matching at the frequency of minimum axial ratio, the quarter-wavelength transformer is connected to the feed stub to transform the impedance looking at the edge of the ring to 50 Ω.

2.5 Results

The prototype antenna operates at about 2.46 GHz. Fig. 7 shows the measured and simulated return loss. However, λ_{gs} is equal to the total length of the antenna (~130mm) at about 2.1 GHz. The shift in the operating frequency can be associated with the length of the microstrip feed stub as discussed in [26].
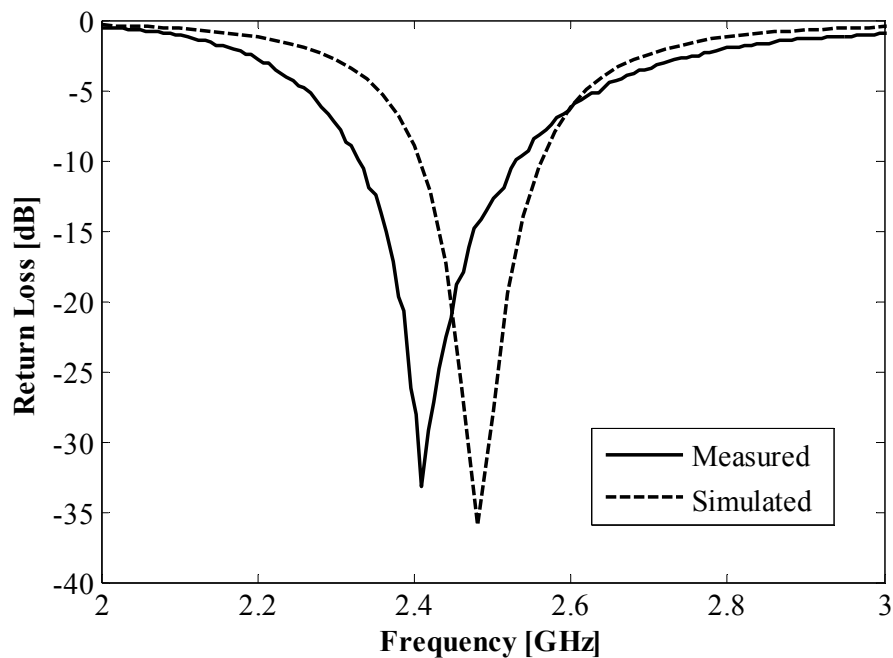
Fig. 7. Measured and simulated return loss.

The axial ratio of the antenna was measured using the *phase amplitude method* [27,28] which is also known as the *linear component method.* In this method, described in [27], a linearly polarized standard gain antenna (SGA) is used to measure both the amplitude and phase along the horizontal and vertical planes (or any two orthogonal cuts) of a CP

radiation pattern. The measured data is stored electronically and then post-processed to find the axial ratio and the gain of the antenna. If E_H and E_V are the complex voltage terms in the horizontal and vertical planes respectively, then at each angle of measurement ψ, the right-hand CP (RHCP) component is given by

$$E_R = \frac{1}{\sqrt{2}}(E_H + jE_V) \tag{10}$$

And the left-hand CP component is given by

$$E_L = \frac{1}{\sqrt{2}}(E_H - jE_V) \tag{11}$$

If $\left|E_R\right| > \left|E_L\right|$ at the main beam angle, then the antenna under test (AUT) is RHCP and $E_R(\psi)$ is the co-polarization pattern, otherwise the AUT is LHCP and $E_L(\psi)$ is the co-polarization pattern.

The polarization purity of a CP antenna is frequently described by specifying its axial ratio (AR). The axial ratio varies from 1 for an ideal CP antenna to ∞ for an ideal linearly polarized (LP) antenna. By measuring a CP antenna's co– and cross-polarization patterns, it is possible to calculate this parameter exactly without the need for additional measurement. If the ratio of E_H and E_V is given by

$$\frac{E_H}{E_V} = ae^{j\delta} \tag{12}$$

Where a is a real number, the axial ratio may then be expressed as

$$AR = \left|\frac{\zeta + 1}{\zeta - 1}\right| \tag{13}$$

Where

$$\zeta = \sqrt{\frac{1 + a^2 + 2a \sin \delta}{1 + a^2 - 2a \sin \delta}} \tag{14}$$

Fig. 8 shows the measured and simulated axial ratio. The measured 3 dB CP bandwidth is about 2.5%. The slight shift in frequency between measured and simulated results can be due to fabrication tolerances and alignment mismatch between the antenna and the feed line.
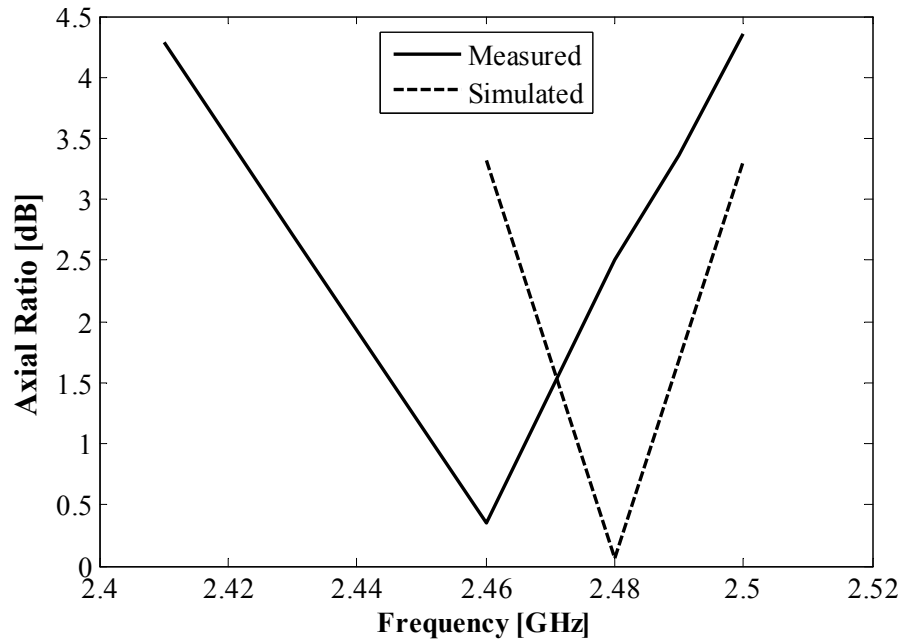
Fig. 8. Measured and simulated axial ratio.

The radiation pattern of the antenna is shown in Fig. 9. Slot antennas usually have a bi-directional pattern. The same is true here, however the pattern is not exactly

symmetrical. This is due to the presence of microstrip feed line on the back of the antenna.
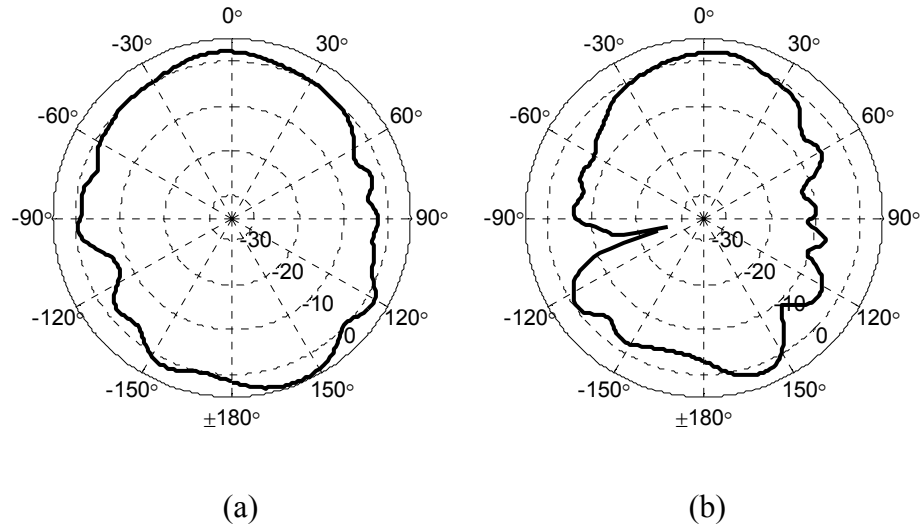
Fig. 9. Measured radiation pattern in dB at 2.46 GHz. (a) x-z plane. (b) y-z plane.

The total gain of a CP antenna can be written as [28]

$$G_T = 10\log_{10}(G_{TV} + G_{TH}) \tag{15}$$

Where G_{TH} and G_{TV} are the partial power gains in the vertical and horizontal planes, respectively.

Fig. 10 shows the measured gain of the antenna in broadside direction. The antenna has a peak gain of about 5.8 dBi in broadside direction.
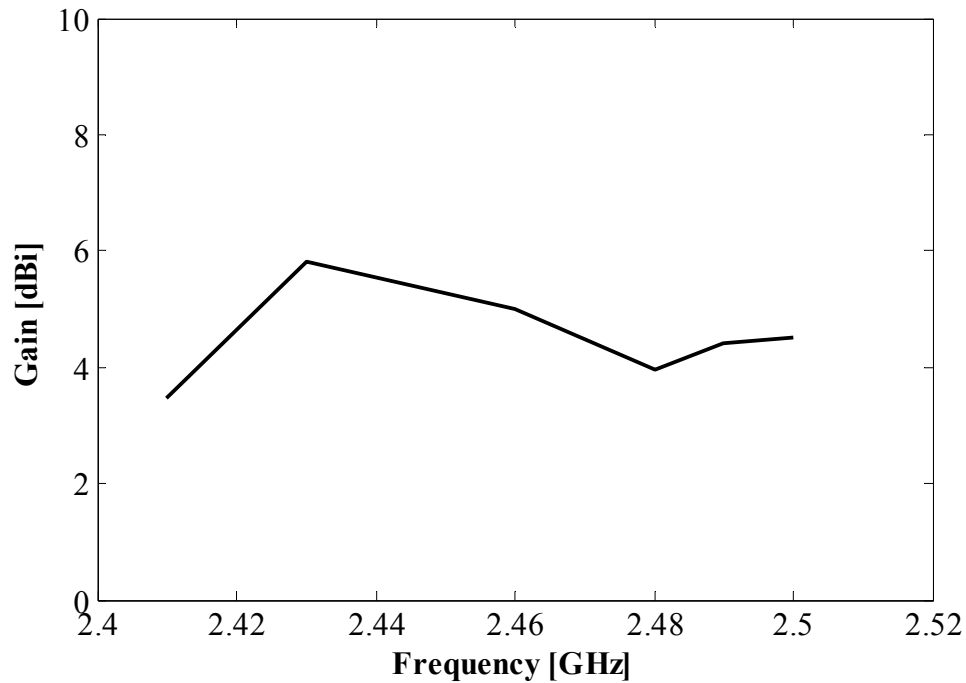
Fig. 10. Measured gain in broadside direction.

2.6 Conclusion

A review of recently reported work on microwave antennas shows that there is a great deal of research being done on designing compact, planar CP antennas. Size is a major design consideration in modern wireless systems. Moreover, CP antennas do not require the alignment between the transmitter and receiver, which can be extremely difficult to do in some cases like satellite communication. Several techniques have been proposed to reduce the size and obtain CP pattern from a single feed microstrip antennas as discussed in this chapter, however slotline antennas have not received much attention in this regard as the microstrip antennas.

The reasons mentioned above were behind the development of the antenna described in this chapter. By using a simple technique, the size of the antenna was reduced by almost half of its conventional counterpart without deteriorating the performance. Comparing with other recently reported slotline antennas [2-4, 24-25], the proposed antenna has high gain of 5.8 dBi. The CP bandwidth is, however, slightly small compared with the CP slot antennas reported in the past, but it can be increased by using a thicker substrate. The key feature of the antenna is its compact size which was the main design objective in this research. The small size of the antenna makes it very attractive for use in modern wireless systems.

CHAPTER III

COMPACT MICROSTRIP BANDPASS FILTER USING

TRIANGULAR OPEN-LOOP RESONATORS

3.1 Introduction

Modern wireless systems require low cost, high performance microwave bandpass filters having low insertion loss, high selectivity and out-of-band rejection. Recent advancement in materials and technologies such as high-temperature superconductors (HTS), micro-machining or microelectromechanical systems (MEMS) and hybrid or monolithic microwave integrated circuits (MMICs) has stimulated the development of new compact microstrip filters [29]. One way to reduce the size of microstrip filters is to use open-loop resonators. Many new microstrip bandpass filter designs have been reported using open-loop resonators such as ring and hairpin resonators. However few designs involved the use of triangular open-loop resonators. Triangular resonators were first introduced by Helszajn and James [30]. However, microstrip filters using triangular resonators have been reported recently [31]. Although the one-dimensional transmission line resonators such as loops and rings are smaller in size than the two-dimensional patch resonators, the loop resonators generally have higher conductor loss and lower power handling capability [31]. Therefore patch resonators are usually preferred for bandpass filter applications where low insertion loss and high power handling are required.

In this research, however, the design of a low loss microstrip three-pole bandpass filter using triangular open-loop resonator is presented. The proposed filter has compact size, low loss and provides good out-of-band rejection. The simulation of the design was carried out using IE3D software. The measured and simulated results show good agreement.

3.2 Review of microstrip bandpass filters using triangular resonators

Triangular resonators were originally introduced by Helszajn and James [30]. It was shown that these resonators have somewhat less radiation loss than the disk resonators and the resultant higher unloaded Q factor for this geometry makes it particularly attractive for use in circulator and filter design. To establish the suitability of triangular resonator for component use, an X-band circulator using triangular resonator was developed and three possible bandpass filter schematics were presented in [30] as shown in Fig.11.

A few years later, Sharma and Bhat [32] reported the analysis of an isosceles triangular microstrip resonator. An isosceles triangular resonator was analyzed with the full wave formulation of the spectral domain technique and a method for evaluating the resonant frequency was presented for a given apex angle and triangle height.

The use of triangular resonators in designing microstrip bandpass filters was first reported by Hong and Lancaster [31]. Two three-pole filters were demonstrated both

(a)

(b)

(c)
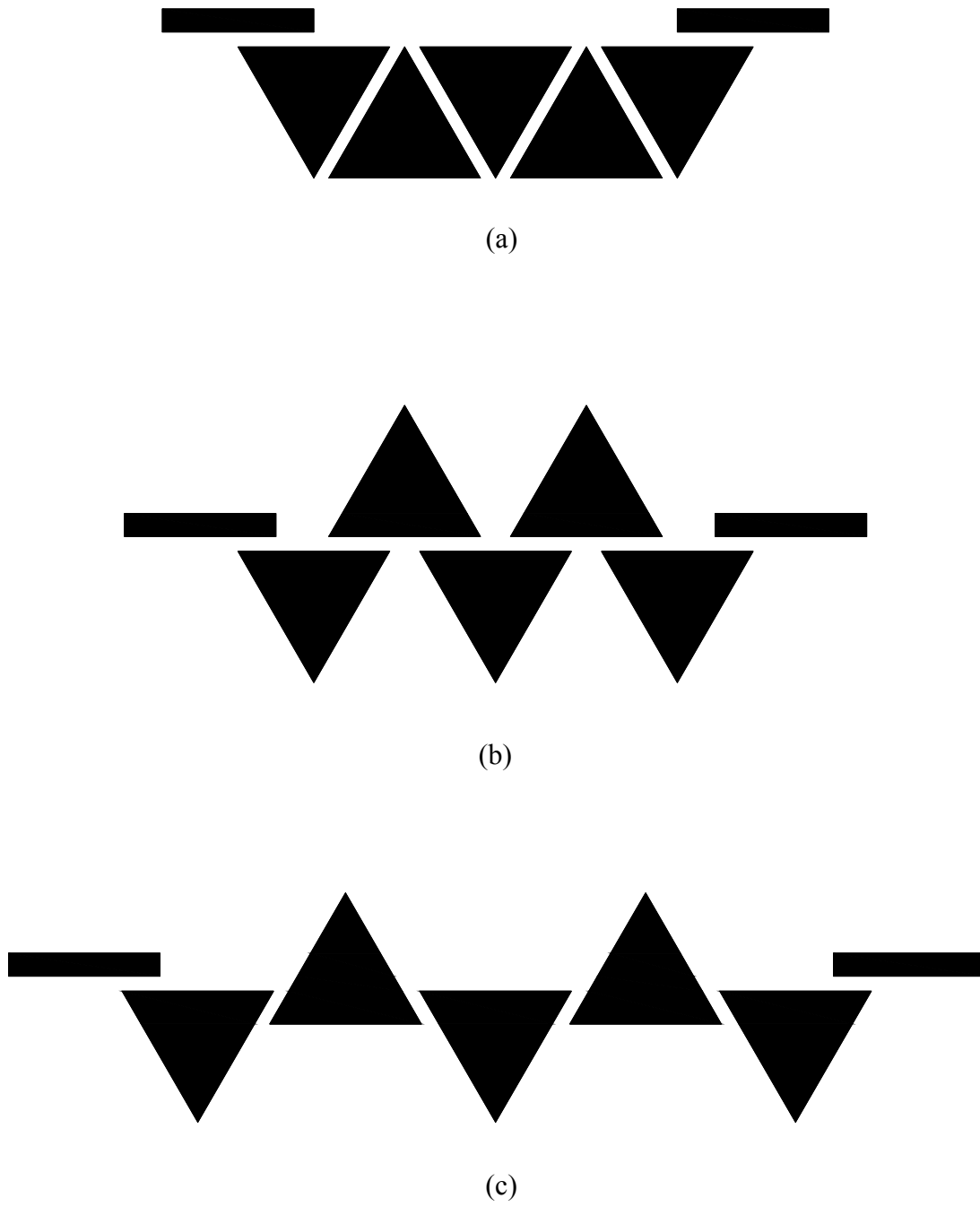
Fig. 11. Bandpass filter schematics using triangular patch resonators [30].

theoretically and experimentally. It was shown that by using two different modes of triangular patch resonators, finite-frequency transmission zeros can be implemented on either side of the passband. The filter structure is similar to that of Fig. 11(a), with three resonators and tapped input and output feed lines. The location of the feed lines can be either along the slant sides or bottom side of the input and output resonator, depending on the operation mode.

The dual-mode operation of a triangular microstrip resonator was investigated first time in [33]. Two- and four-pole bandpass filters were demonstrated both theoretically and experimentally [33,34]. The dual mode operation was obtained by either introducing a small cut in the equilateral triangle resonator or by deforming the equilateral triangle resonator into an isosceles triangle. The reported four-pole bandpass filter, shown in Fig. 12, has a measured insertion loss of ~2.3 dB at a midband frequency of 4.01 GHz.

Fig. 12. Four-pole dual-mode microstrip triangular patch resonator filter [33].

The use of triangular loop resonator in microstrip bandpass filter was reported in [35]. A four-pole bandpass filter based on triangular open-loop resonator was proposed as shown in Fig. 13. The center frequency of the bandpass filter is 1.95 GHz and the bandwidth is 60 MHz. This filter provides improved selectivity characteristics with narrow bandwidth and compact size.
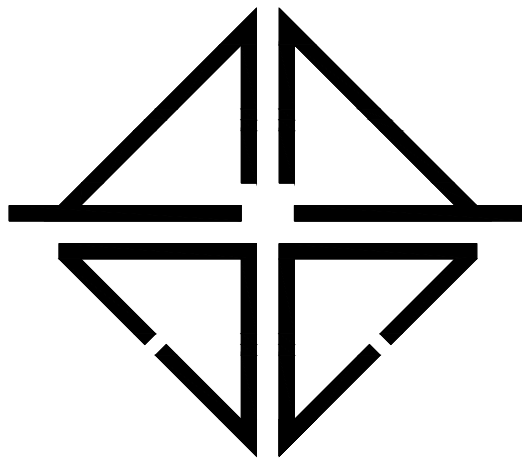
Fig. 13. Four-pole microstrip triangular open-loop resonator filter [35].

Microstrip triangular patch resonator filters with two transmission zeros were proposed in [36]. The two transmission zeros on either side of the passband are obtained by creating asymmetry in the structure. This can be done by using an asymmetrical feed lines, as shown in Fig. 14(a), or by using scalene triangular resonators as shown in Fig. 14(b). By placing circular and triangular notches in the structure as shown in Fig. 14(c)

and Fig. 14(d) respectively, the center frequency and the bandwidth of the filter can also be controlled [36].

(a) (b)

(c) (d)
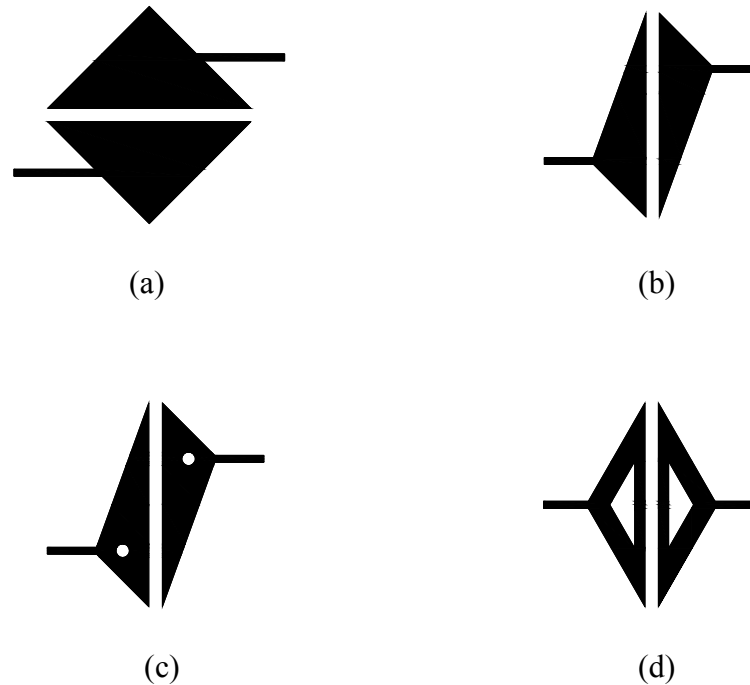
Fig. 14. Triangular patch resonator filters with two transmission zeros [36].

Another dual-mode microstrip bandpass filter design using slotted triangular patch resonator was reported in [37]. Dual mode operation is obtained by adding one traverse and two longitudinal slots to the equilateral triangular patch as shown in Fig. 15. The midband frequency of the proposed two-pole dual mode filter is 3.94 GHz with fractional bandwidth of 4.3 %. The filter has an insertion loss of about 2.3 dB and return loss of larger than 20 dB in the passband.

Fig. 15. Slotted dual-mode equilateral triangle patch resonator [37].

A microstrip bandpass filter design using dual-mode triangular loop resonator was presented for the first time in [38]. The filter shows 8 % bandwidth with insertion loss ranging from 0.82 dB to 1.4 dB at 10 GHz depending on the perturbation arrangement. The different perturbation arrangements for dual-mode operation are in the form cuts and patches on the three corners of the equilateral triangular resonator as shown in Fig. 16.

The above discussion shows that triangular resonators have certain advantages over other resonators of different geometry mainly circular and square. They have higher Q which is attractive for filter design. They provide easy method for placing transmission zeros in filter response. They can be easily edge-coupled with each other as oppose to circular resonators and they make the use of circuit space more efficiently than square resonators thereby making the circuits more compact.

(a)

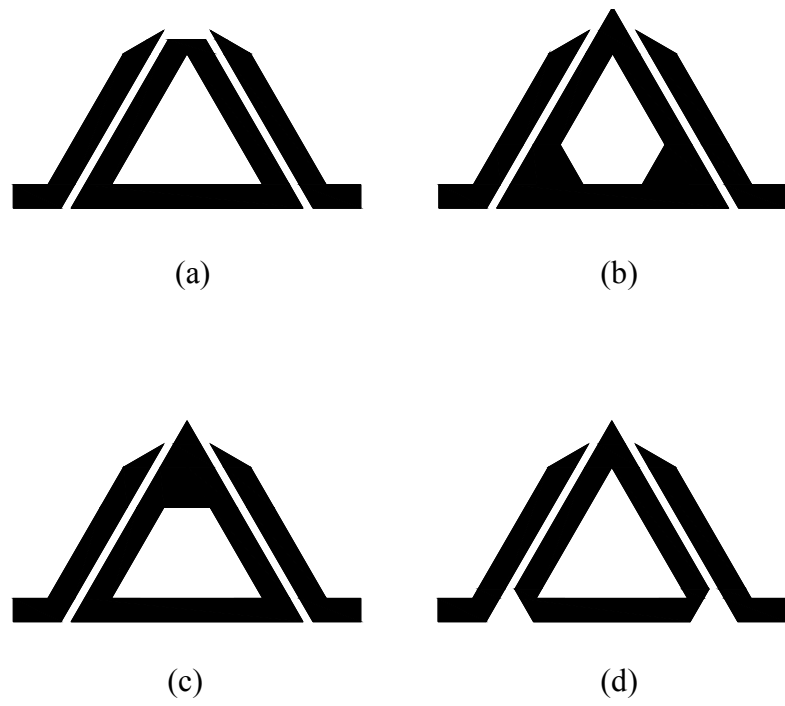(b)

(c)

(d)

Fig. 16. Bandpass filter using dual-mode microstrip triangular loop resonator [38].

3.3 Filter design

The proposed bandpass filter is shown in Fig. 17 along with actual dimensions. The filter consists of four triangular open-loop resonators in a cross-coupled structure. Each resonator has the dimensions of an isosceles right triangle with two sides of equal length $a/\sqrt{2}$, where a is the length of the third side. The fourth resonator is placed to improve the cross coupling between the resonators which gives a better skirt rejection [39], so the proposed filter is basically two three-pole bandpass filters in parallel. The coupling gap between adjacent resonators is G, and S is the distance between the two open ends of each triangular resonator. The filter design is based on the coupling coefficients of intercoupled resonators and the external quality factors of the input and output resonators. In this structure, there are four coupling coefficients to be determined, namely k_{12}, k_{23}, k_{14}, and k_{34}, where k_{ij} specifies the coupling between resonators i and j. Since all the coupling coefficients are identical as can be seen from the structure, let all the coupling coefficients be equal to k. Q_e is the external quality factor of the input and output resonator. The filter is designed to meet the specifications shown in Table 2.

Table 2: Bandpass filter specifications

Fraction bandwidth (FBW)	0.07 or 7%
Center Frequency	2.8 GHz
Filter response type	Chebyschev
Number of poles	3
Pass-band ripple	0.1 dB
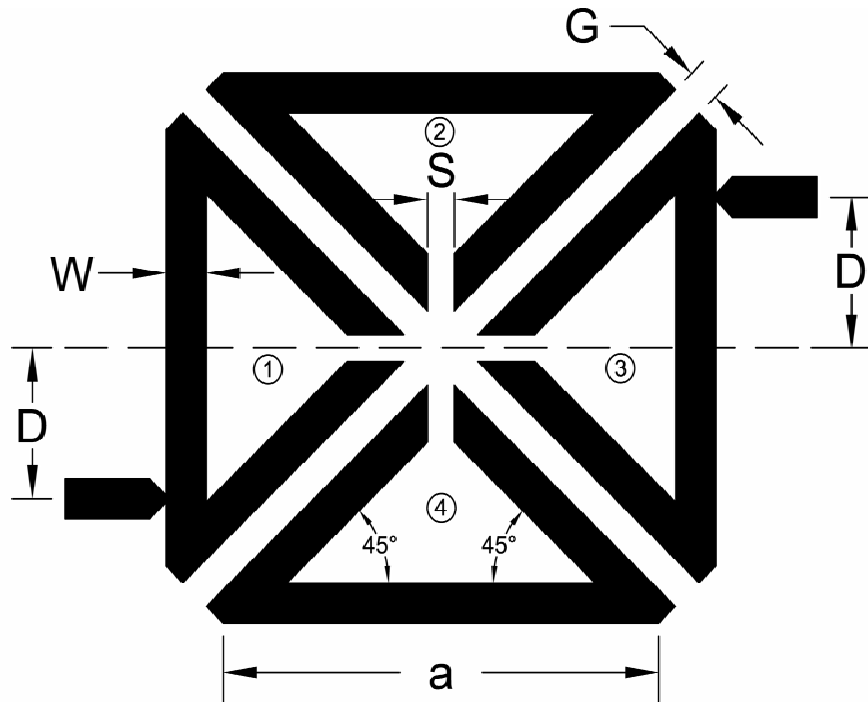
Fig. 17. Geometry of the proposed bandpass filter: W=1.8 mm, S=0.2 mm, D=3 mm, G=0.9 mm and a= 12 mm.

The element values g_i for the given three pole Chebyschev lowpass prototype are $g_0=g_4=1$, $g_1=g_3=1.0316$ and $g_2=1.1474$ [29]. The external quality factor and the coupling coefficients of the proposed filter can then be found by [29]

$$Q_e = \frac{g_0 g_1}{FBW} \tag{16}$$

$$k = \frac{FBW}{\sqrt{g_1 g_2}} \tag{17}$$

Where FBW is the fractional bandwidth of the filter. Thus $k=0.06$ and $Q_e=14.7$

Shown in Fig. 18 is a typical resonant frequency response of two coupled triangular resonators. The measured coupling coefficient is given by [29]

$$k = \frac{f_{p2}{}^2 - f_{p1}{}^2}{f_{p2}{}^2 + f_{p1}{}^2} \qquad (18)$$

where f_{p1} and f_{p2} are the lower and upper resonant frequencies of the resonator. Fig. 19 shows the measured coupling coefficient for various coupling gaps between the resonators. The graph shows that a coupling gap of about 0.9 mm gives the required coupling coefficient between the resonators.
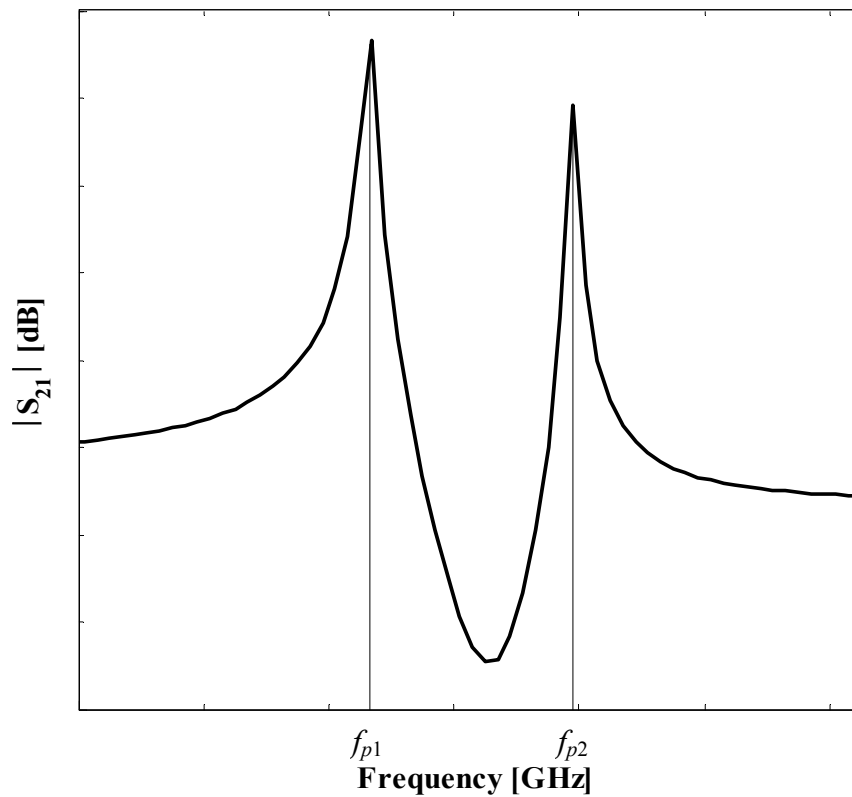
Fig. 18. Typical resonant response of two coupled triangular resonators.
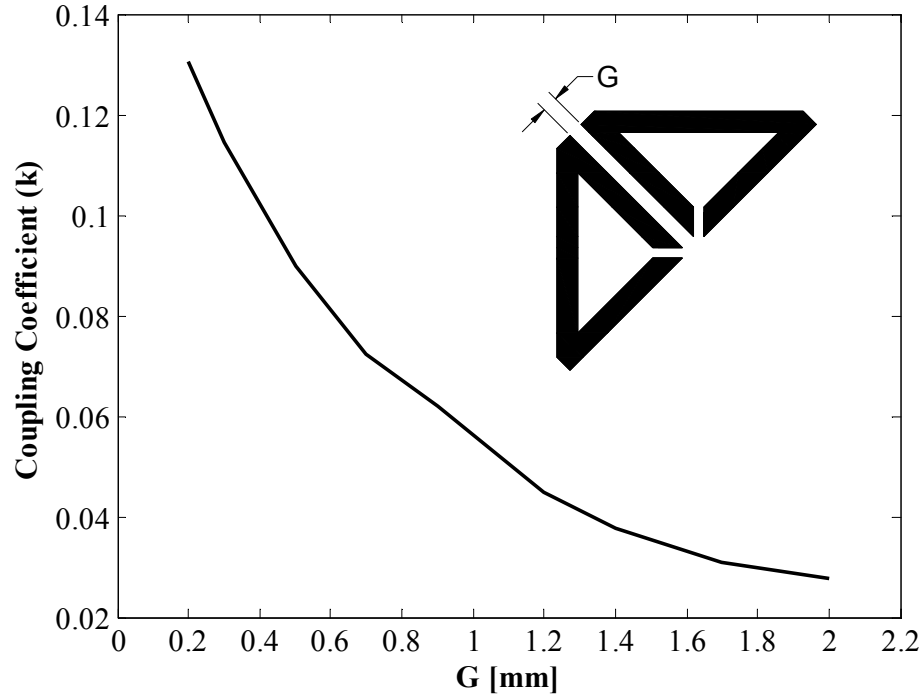
Fig. 19. Coupling coefficient for various coupling gaps.

Shown in Fig. 20 is a typical plot of $|S_{21}|$ versus frequency for the triangular resonator. At resonance, $|S_{21}|$ reaches its maximum value $|S_{21}(f_o)|$. Fig. 21 shows the measured external quality factor against the input and output tapping positions. The measured singly loaded external quality factor is given by

$$Q_e = \frac{2f_o}{\Delta f_{3\ dB}}$$
(19)

Where f_o is the resonant frequency and $\Delta f_{3\text{-}dB} = f^+_{3\text{-}dB} - f^-_{3\text{-}dB}$ is the bandwidth at which the attenuation for S_{21} is up 3 dB from that at resonance. From graph, an offset of 3 mm in the tapping positions gives the required quality factor.
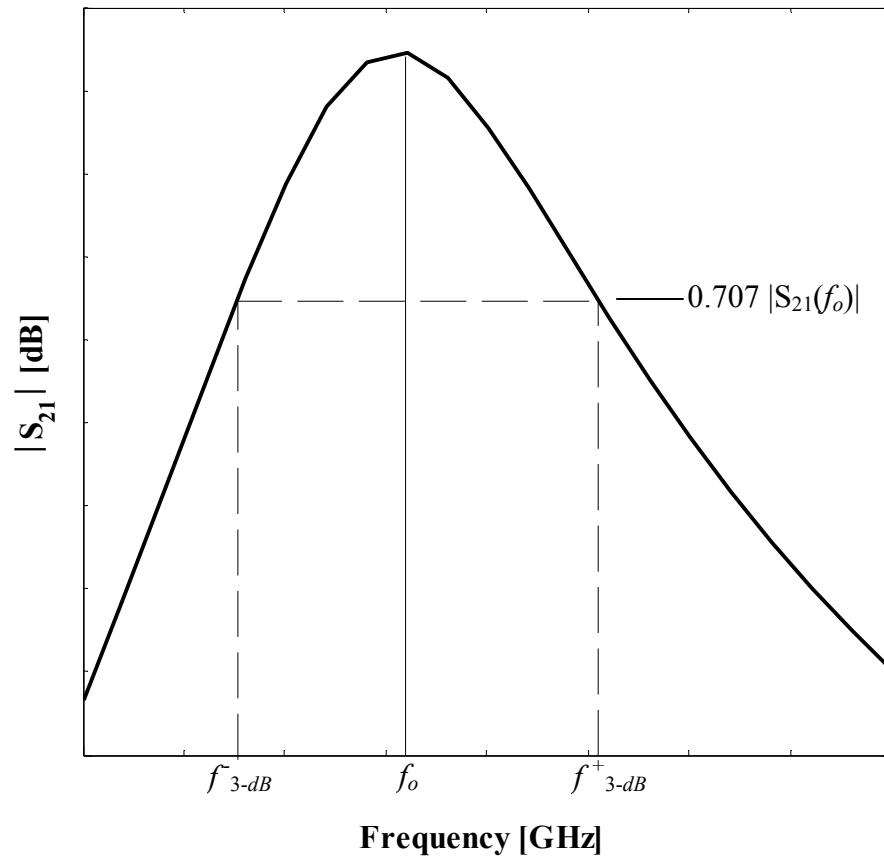
Fig. 20. Typical resonant amplitude response of S_{21} for the triangular resonator.
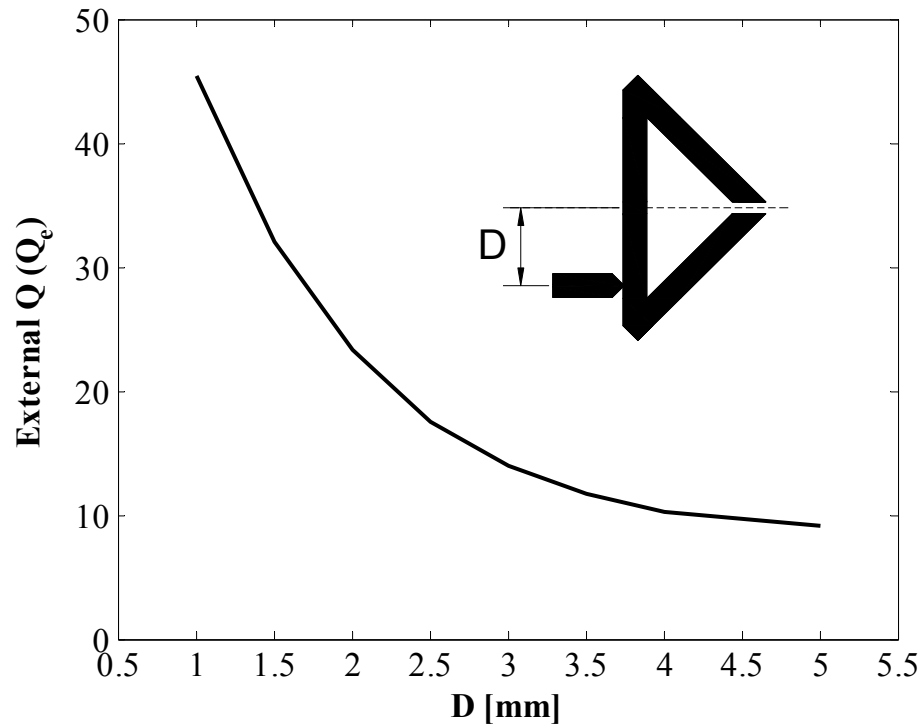
Fig. 21. External quality factor for various input and output tapping positions.

3.4 Results

The new compact three-pole bandpass filter is fabricated on Rogers RT\duroid 6010 with dielectric constant ε_r=10.8 and thickness h=75 mils. The actual dimensions of the filter shown in Fig. 17 are: W=1.8 mm, S=0.2 mm, D=3 mm, G=0.9 mm and a= 12 mm. Fig. 22 shows the measured and simulated return loss and insertion loss. The filter has insertion loss of less than 1 dB and return loss of more than 15 dB in the passband. The passband of the filter is from 2.75 GHz to 2.95 GHz. The slight difference in frequency between the results can be due to fabrication tolerances. The filter has one transmission zero in the lower stop band at about 2.4 GHz with 44 dB rejection. The maximum

rejection of around 42 dB occurs in the upper stop band at about 3.65 GHz. The overall

out-of-band rejection is better than 30 dB from 1.5 to 2.5 GHz and 3.2 to 4.2 GHz.
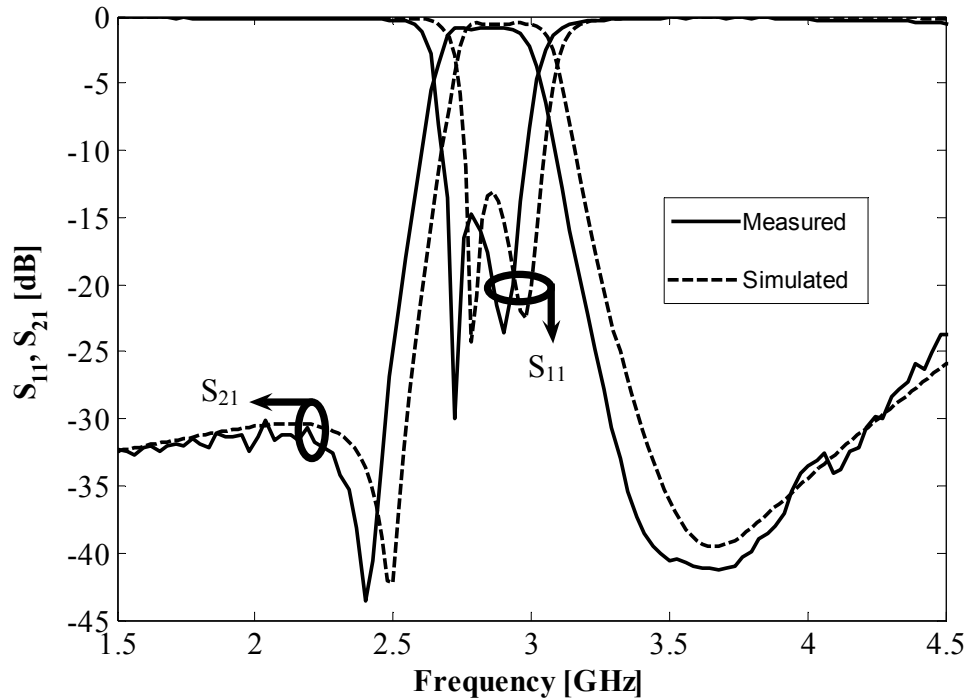
Fig. 22. Measured and simulated results of the three-pole bandpass filter.

3.5 Conclusion

A review of microstrip bandpass filter designs reported in the past shows that relatively

few filter designs involved the use of microstrip triangular resonator. Triangular

resonator has inherent advantages due to its geometry which give a designer greater

flexibility in designing microwave circuits. It provides easy edge coupling between

resonators as compared to ring or disc resonators, and it utilizes the circuit space more

efficiently then square ring or patch resonators thereby making the circuits more compact.

The design of a new three-pole microstrip bandpass filter based on triangular resonators was described. The filter consists of four triangular open-loop resonators in a cross-coupled structure which gives a better skirt rejection. The proposed filter has low insertion loss of less than 1 dB and good out-of-band rejection. The small size of the filter makes it very suitable for use in modern microwave integrated circuits.

CHAPTER IV

SUMMARY AND RECOMMENDATIONS

4.1 Summary

Modern RF/microwave wireless systems require high performance, low cost and small size circuits. A great deal of research carried out recently dealt with the miniaturization of microwave circuits, and it is quite obvious that in future also, circuit size will be a major design consideration. In other words, techniques to reduce the size of microwave circuits without compromising on the performance will be a major area of research. Moreover, planar transmission-line (microstrip, slotline, CPW etc.) circuits are receiving much attention as they are easily compatible with microwave integrated circuits (MICs) and monolithic microwave integrated circuits (MMICs). This thesis comprises two research topics, both involving the design of compact microwave circuits.

The first topic of this thesis is the design of a miniaturized, circularly polarized (CP) slot-ring antenna. In this research, it is shown that the size of a conventional CP slot-ring antenna is reduced by about 50 % by introducing meandered slot sections in the ring. The meandered sections occupy the inner area of the ring, thus utilizing the space more efficiently. The antenna displays a CP bandwidth of about 2.5 % and has a peak gain of 5.8 dBi in the broadside direction.

The second topic involves the design of a compact three-pole microstrip bandpass filter using triangular open-loop resonators. The filter comprises four triangular open-loop resonators in a cross–coupled structure to provide better skirt rejection. The filter displays low insertion loss of less than 1 dB in the passband centered at 2.85 GHz. The proposed filter has 7% bandwidth and an out-of-band rejection of greater than 30 dB from 1.5 to 2.5 GHz and 3.2 to 4.2 GHz.

4.2 Recommendations

Other feed configurations discussed in chapter II should also be considered for the proposed slot-ring antenna. Slotline feed provides inductive coupling to the slotline ring which is more efficient at lower frequencies. Also one can have a completely planar circuit using CPW or slotline feeds for the proposed antenna. The CP bandwidth of the antenna can also be increased by using a thicker substrate.

The use of triangular resonators in designing RF/microwave circuits needs more attention. Triangular resonator has inherent advantages due to its geometry which give a designer greater flexibility in designing microwave circuits. It provides easy edge coupling between resonators as compared to ring or disc resonators, and it utilizes the circuit space more efficiently then square ring or patch resonators thereby making the circuits more compact. Along with triangular microstrip resonator, triangular slot and CPW resonators should also be explored.

REFERENCES

[1]   K.-L. Wong, C.-C. Huang, and W.-S. Chen, "Printed ring slot antenna for circular polarization," *IEEE Trans. Antennas Propagat.*, vol. 50, no. 1, pp. 75-77, Jan. 2002.

[2]   J.-S. Row, "The design of a square-ring slot antenna for circular polarization," *IEEE Trans. Antennas Propagat.*, vol. 53, no. 6, pp. 1967-1972, June 2005.

[3]   J.-S. Row, C. Y. D. Sim, and K.-W. Lin, "Broadband printed ring-slot array with circular polarization," *Electron. Lett.*, vol. 41, no. 3, pp. 110-112, Feb. 2005.

[4]   K. Chang, L.-H. Hsieh, *Microwave Ring Circuits and Related Structures*. 2nd ed., Hoboken, New Jersey: Wiley, 2004.

[5]   K. Kawano and H. Tomimuro, "Slot ring resonator and dispersion measurement on slot lines," *Electron. Lett.*, vol. 17, no. 24, pp. 916-917, November 26, 1981.

[6]   K. D. Stephan, N. Camilleri, and T. Itoh, "A quai-optical polarization-duplexed balanced mixer for millimeter-wave applications," *IEEE Trans. Microwave Theory Tech.*, vol. MTT-31, no.2, pp. 164-170, February 1983.

[7]   J. Navarro and K. Chang, "Varactor-tunable uniplanar ring resonators," *IEEE Trans. Microwave Theory Tech.*, vol. MTT-41, no. 5, pp. 760-766, May 1993.

[8]   K. Kawano and H. Tomimuro, "Spectral domain analysis of an open slot ring resonator," *IEEE Trans. Microwave Theory Tech.*, vol. MTT-30, no. 8, pp. 1184-1187, August 1982.

[9]   G. Dubost, "Theoretical radiation resistance of an isolated slot ring resonator," *Electron. Lett.*, vol. 23, no. 18, pp. 928-930, August 27, 1987.

[10]   I. Wolff, "Microstrip bandpass filter using degenerate modes of a microstrip ring resonator," *Electron. Lett.*, vol. 8, no. 12, pp. 302-303, June 15, 1972.

[11]   H. Nakano, K. Vichien, T. Sugiura, and J. Yamauchi, "Singly-fed patch antenna radiating a circularly polarized conical beam," *Electron. Lett.*, vol. 26, no. 10, pp. 638-640, May 1990.

[12]   A. K. Bhattacharyya and L. Shafai, "A wider band microstrip antenna for circular polarization," *IEEE Trans. Microwave Theory Tech.*, vol. 36, no. 2, pp. 157-163, February 1988.

[13]   R. R. Ramirez, F. D. Flaviis, and N. G. Alexopoulos, "Single-feed circularly polarized microstrip ring antenna and arrays," *IEEE Trans. Antennas Propagat.*, vol. 48, no. 7, pp. 1040-1047, July 2000.

[14]   P. C. Sharma and K. C. Gupta, "Analysis and optimized design of single feed circularly polarized microstrip antenna," *IEEE Trans. Antennas Propagat.,* vol. AP-31, no. 6, pp. 949-955, November 1983.

[15]   W.-S. Chen, C.-K. Wu, and K.-L. Wong, "Square-ring microstrip antenna with a cross strip for compact circular polarization operation," *IEEE Trans. Antennas Propagat.,* vol. 47, no. 10, pp. 1566-1568, October 1999.

[16]   W.-S. Chen, C.-K. Wu, and K.-L. Wong, "Single-feed square-ring microstrip antenna with truncated corners for compact circular polarization operation," *Electron. Lett.*, vol. 34, no. 11, pp. 1045-1047, May 1998.

[17] W.-S Chen and H.-D Chen, "Single-feed circularly polarized square-ring microstrip antennas with a slit," in *IEEE AP-S Int. Symp. Digest*, vol. 3, pp. 1360-1363, June 1998.

[18] C. Y. D. Sim, K.-W. Lin, and J.-S. Row, "Design of an annular-ring microstrip antenna for circular polarization," in *IEEE AP-S Int. Symp. Digest*, vol. 1, pp. 471-474, June 2004.

[19] H. Iwasaki, "A circularly polarized small-size microstrip antenna with a cross slot," *IEEE Trans. Antennas Propagat.*, vol. 44, no. 10, pp. 1399-1401, October 1996.

[20] S. A. Bokhari, J.-F. Zurcher, J. R. Mosig, and F. E. Gardiol, "A small microstrip patch antenna with a convenient tuning option," *IEEE Trans. Antennas Propagat.*, vol. 44, no. 11, pp. 1521-1528, November 1995.

[21] K.-L. Wong and J.-Y. Wu, "Single-feed small circularly polarized square microstrip antenna," *Electron. Lett.*, vol. 33, no. 22, pp. 1833-1834, October 1997.

[22] W.-S. Chen, C.-K. Wu, and K.-L. Wong, "Novel compact circularly polarized square microstrip antenna," *IEEE Trans. Antennas Propagat.*, vol. 49, no. 3, pp. 340-342, March 2001.

[23] W.-S. Chen, K.-L. Wong, and C.-K. Wu, "Inset microstripline-fed circularly polarized microstrip antennas," *IEEE Trans Antennas Propagat.,* vol. 48, no. 8, pp. 1253-1254, August 2000.

[24] M. L. Wong, H. Wong, and K.-M. Luk, "Small circularly polarized patch antenna," *Electron. Lett.*, vol. 41, no. 16, August 2005.

[25] H. A. Ghali and T. A. Moselhy, "Broad-band and circularly polarized space-filling-based slot antennas," *IEEE Trans. Microwave Theory Tech.*, vol. 53, no. 6, pp. 1946-1950, June 2005.

[26] H. Terhrani and K. Chang, "Multifrequency operation of microstrip-fed slot-ring antennas on thin low-dielectric permittivity substrates," *IEEE Trans. Antennas Propagat.*, vol. 50, no. 9, pp. 1299-1308, September 2002.

[27] C. T. Rodenbeck, K. Chang and, J. Aubin, "Auotmated pattern measurement for circularly-polarized antennas using the phase-amplitude method," *Microwave Journal*, vol. 47, no. 7, pp. 68-78, July 2004.

[28] C. A. Balanis, *Antenna Theory Analysis and Design*. 3rd ed., Hoboken, New Jersey: Wiley, 2005.

[29] J.-S. Hong and M. J. Lancaster, *Microstrip Filters for RF/Microwave Application.* New York, New York: Wiley, 2001.

[30] J. Helszajn and D. S. James, "Planar triangular resonators with magnetic walls," *IEEE Trans. On Microwave Theory Tech.*, vol. MTT-26, no. 2, pp. 95-100, February 1978.

[31] J.-S. Hong and M. J. Lancaster, "Microstrip triangular patch resonator filters," in *IEEE MTT-S Int. Symp. Digest*, vol. 1, pp. 331-334, June 2000.

[32] A. K. Sharma and B. Bhat, "Analysis of triangular microstrip resonators," *IEEE Trans. Microwave Theory Tech.*, vol. 30, no. 11, pp. 2029-2031, November 1982.

[33] J.-S. Hong and S.Li, "Dual-mode microstrip triangular patch resonators and filters," in *IEEE MTT-S Int. Microwave Symp. Digest.*, vol. 3, pp. 1901-1904, June 2003.

[34] J.-S. Hong and S. Li, "Theory and experiment of dual-mode microstrip triangular patch resonator filters," *IEEE Trans. Microwave Theory Tech.*, vol. 52, no. 4, pp. 1237-1243, April 2004.

[35] S. Chaimool, S. Kerdsumang, and P. Akkaraekthalin, "A novel microstrip bandpass filter using triangular open-loop resonators," in *9th Asia-Pacific Comm. Conf.*, vol. 2, pp. 788-791, September 2003.

[36] X. Wang and Y. Li, "New microstrip patch resonators filters with two transmission zeros," in *Asia-Pacific Environmental Electromagnetics Conf.*, pp. 364-368, November 2003.

[37] W. Hu, Z. Ma, D. Xu, Y. Kobayashi, T. Anada, and G. Hagiwara, "Microstrip bandpass filter using degenerate dual-modes of slotted equilateral triangular patch resonators," in *Proc. Asia-Pacific Microwave Conf.*, vol. 1, December 2005.

[38] C. Lugo and J. Papapolymerou, "Bandpass filter design using a microstrip triangular loop resonator with dual-mode operation," *IEEE Microwave Wireless Comp. Lett.*, vol. 15, no. 7, pp. 475-477, July 2005.

[39] K. T. Jokela, "Narrow-band stripline or microstrip filters with transmission zeros at real and imaginary frequencies," *IEEE Trans. Microwave Theory Tech.*, vol. MTT-28, no. 6, pp. 542-547, June 1980.

VITA

Muhammad Fahad Farooqui received his Bachelor of Engineering degree in electronics from the NED University of Engineering and Technology, Karachi in January, 2003. After graduating, he joined the Institute of Space Technology, Karachi, Pakistan, where he worked as assistant manager on the design and development of various transmitter/receiver modules of a communication satellite. He started pursuing his M.S. degree in electrical engineering at Texas A&M University under the supervision of Dr. Kai Chang in January, 2005. His research interests include RF/microwave circuits and electromagnetics. Fahad's permanent address is C-19, Block-17, Gulshan-e-Iqbal, Karachi-75300, Pakistan.